Dynamic torsional unwinding of southern pine tracheids as observed in the scanning electron microscope

CHARLES W. McMILLIN, U.S. Department of Agriculture, Forest Service, Pineville, USA

KEYWORDS: Mechanical pulps, Chip groundwood, Tracheids, Cell structure, Mechanical properties, Southern pines, *Pinus taeda*.

SUMMARY: In previous research on the process for making groundwood in a double-disk refiner, a theoretical stress analysis indicated that tracheids of *Pinus taeda L.* may fail while under torsional stress and unwind into ribbonlike elements. Such elements provide the coherence necessary for strength development in these pulps. Depending upon their physical state, tracheids may also buckle or shear and yield no ribbons.

In this study, macerated earlywood and latewood tracheids of loblolly pine were stressed in torsion with a specially designed fixture and observed at high magnification in a scanning electron microscope. Three previously postulated failure types were identified. Type I was characterized by the formation of a crack, generally parallel to the zone of weakness delineated by the fibril helix, followed by unwinding into a ribbon with further twisting. Type II failures were by shear perdendicular to the fiber axis, while Type III were by continuous diagonal buckling.

For earlywood fibers rotated in a clockwise direction, the proportion of Type I (unwinding) failures decreased with increasing axial separation (the distance between the points of applied torque). The proportion was unaffected when tracheids were heated to about 100°C. In latewood, the proportion of Type I failures increased with axial separation when tested at 20°C, but remained relatively constant with increasing separation when tested at 100°C; for a given separation, the proportion was greater for hot than for cold fibers. For the test conditions, total length of the ribbonlike portion was generally shorter for latewood than for earlywood.

For both earlywood and latewood, the proportion of Type II failures was greatest when the axial separation was small and the fibers were unheated. Type III failures were principally associated with wide axial separation. Counterclockwise rotation of the fiber proved undesirable, since no Type I failures were generated.

It was also observed that removal of the S_1 layer prior to application of torsional stresses aided development of ribbonlike elements.

☐ I tidigare undersökningar rörande framställning av mekanisk massa i dubbelskiveraffinör visades teoretiskt, att trakeider av *Pinus taeda L.* kan lindas upp i bandliknande element, om de belastas med torsionskrafter. Dessa element ger den sammanhållning som bestämmer styrkeutvecklingen i massan. Trakeiderna kan också skjuvas av eller buckla sig beroende på deras fysikaliska tillstånd.

I denna undersökning har i vatten särade och sedan torkade vårveds- och höstvedstrakeider från Lobolly pine utsatts för torsion i en speciell anordning, samtidigt som de har observerats i ett svepelektronmikroskop med hög grad av förstoring. Tre tidigare postulerade brottyper kunde observeras. Brottyp I karakteriserades av en sprickbildning, vanligen parallell med de svaga områdena längs fibrillspiralen. Vid ytterligare torsion uppstod en avlindning i bandliknande element. Brottyp II åstadkoms av skjuvkrafter vinkelräta mot fiberaxeln, medan brottyp III bildades genom fortskridande buckling av fibern.

För vårvedsfibrer, som vreds medurs minskade andelen av brottyp I (avlindning) med ökat inspänningsavstånd (avståndet mellan torsionskrafternas angreppspunkter). Denna andel påverkades inte av uppvärmning av fibrerna till omkring 100°C. För höstvedsfibrer ökade andelen av brottyp I med inspänningsavståndet, när fibrerna testades vid 20°C, medan denna andel var relativt oberoende av inspänningsmotståndet vid 100°C. Vid givet inspänningsavstånd var andelen av brottyp I större för varma än för kalla fibrer. Den totala längden av de bandlika elementen var vanligen kortare för höstveds- än för vårvedsfibrer.

För både höstveds- och vårvedsfibrer gällde, att andelen av brottyp II var större, när inspänningsavståndet var litet och fibrerna ouppvärmda. Brottyp III inträffade företrädesvis vid stort inspänningsavstånd. Torsion moturs av fibrerna visade sig vara ogynnsam, då ingen brottyp I åstadkoms.

Vid undersökningen framkom även, att jämförelsevis flera bandliknande element bildades efter S_1-skiktets borttagande.

☐ Es wurde in einer früheren Untersuchung über die Herstellung von Holzschliff mit einem Doppelscheiben-Refiner theoretisch vorausgesagt, dass unter dem Einfluss von Torsionskräften die Tracheiden von *Pinus taeda L.* verstaucht und in bandförmige Elemente entrollt werden könnten. Solche Elemente bewirken den Zusammenhalt der für die Festigkeitsentwicklung dieser Zellstoffe erforderlich ist. In Abhängigkeit vom physikalischen Zustand können die Tracheiden auch geknickt oder verschubt werden und liefern dann keine Bändchen.

In dieser Untersuchung wurden in einer speziellen Anordnung durch Mazeration isolierte Früh- und Spätholztracheiden der Loblolly-Kiefer einer Torsionsbehandlung unterworfen und gleichzeitig bei hoher Vergrösserung im Rasterelektronenmikroskop untersucht. Drei bereits früher postulierte Schädigungstypen wurden festgestellt: Typ I wird charakterisiert durch Rissbildung — im Allgemeinen parallel zur Lockerzone, die der Fibrillenschraubung folgt — durch welche bei weiterer Verdrillung sich Bänder abwickeln. Schädigungstyp II besteht in einem Schub senkrecht zur Faserachse, während Typ III einen schräg zur Faserachse kontinuierlichen Knick darstellt.

Bei Frühholzfasern, die im Uhrzeigersinn gedreht sind, nimmt der Anteil an Typ I (Bändchenabwicklung) mit zunehmender Einspannlänge (Abstand zwischen den Angriffspunkten der Torsion) ab. Das Ausmass war unverändert bei einer Erwärmung der Tracheiden bis auf etwa 100°C. In Spätholztracheiden nimmt bei 20°C der Anteil an Schäden vom Typ I mit steigender Einspannlänge jedoch zu; bei einer Testung bei 100°C blieb aber der Anteil relativ konstant, wenn die Einspannlänge vergrössert wurde. Bei gegebener Einspannlänge war der Anteil grösser für erwärmte als für kalte Fasern. Unter den gewählten Bedingungen war die Totallänge der bändchenförmigen Elemente kurzer für Spätholz- als für Frühholzzellen.

Für beide Faserarten war der Schädigungstyp II am ausgeprägtesten, wenn die Einspannlänge klein und die Fasern nicht erwärmt waren. Schädigungstyp III war hauptsächlich an grosse Einspannlängen gebunden. Verdrillungen gegen den Uhrzeigersinn erwiesen sich ungünstig, da kein Schädigungstyp I erzeugt wird.

Es wurde auch beobachtet, dass die vorherige Entfernung der S_1-Schicht die Ausbildung bändchenförmiger Elemente beim Torsionsangriff begünstigt.

ADDRESS OF THE AUTHOR: Southern Forest Experiment Station, 2500 Shreveport Highway, Pineville, Louisiana 71360, USA.

Problems of industrial pollution coupled with increasing demands for conservation of the wood resource have accelerated the search for a high-strength mechanical pulp that could be used to reduce or eliminate chemical pulps in some applications. At present, the direct reduction of chips in disk refiners is generally held to offer the best opportunity to achieve this goal.

While refiner groundwood pulps of good strength and runability on paper machines have been manufactured from some western species (1), the wood of the southern pines appears to present a greater challenge. For example, trials with commercial refiners have not yielded pulp of sufficient strength. Examination of these pulps suggests that their low strength is partly caused

by a deficiency in bonding potential (2). Forgacs (3) stated that the problem could be resolved by unravelling a higher proportion of the relatively thick-walled tracheids of southern pine into ribbonlike particles. Could this be accomplished, substantial improvement in sheet strength would be expected since such ribbons are highly flexible and deformable—a condition favoring hydrogen bonding. McMillin (4) has suggested that the desired ribbonlike elements are derived by an unwinding process after the parent tracheid has been stressed in torsion during refining.

The study reported here sought to identify, by direct observation in a scanning electron microscope, the failure mechanism of intact southern pine *(Pinus taeda L.)* tracheids when subjected to torsional stress and elucidate some of the factors influencing such failures.

The torsion model

Although an exact theoretical model is confounded by thermo- and hydrodynamic effects and the anisotropic nature of fibers, an approximation developed in earlier studies (4) demonstrates, in terms of improved sheet strength, an interaction between torsional forces within an intact fiber and the morphological characteristics of the fiber. Briefly summarized, the model is as follows.

Consider a uniform, smooth-sided, right-cylindrical, intact fiber consisting of only the S_2 layer and having outside diameter d_o, inside diameter d_i, and length L. Assume that during the latter phases of refining the fiber becomes radially aligned (5) between the surfaces of two counter-rotating disks of radius R revolving at speed S *(fig. 1A)*. If there is no slippage, the fiber tends to rotate about its longitudinal axis $X—X'$ at a velocity proportional to the rotational velocity of the disk at distance R' from the disk center. Because the velocity of the disk varies directly with the disk radius, the rotational velocity of the fiber is slightly greater at point B' than at point B, and the fiber is acted upon by a couple of equal numerical moment but with opposite sign. Under these conditions, the fiber may be analyzed as a hollow circular shaft stressed in torsion.

If the undeformed fiber is considered to be held in mechanical equilibrium, *fig. 1B* approximates the force relationship within it. Under torsion, the shaft is twisted by a couple $P—P'$. The magnitude of the couple will be a function of the difference between the rotational velocities at distance L apart. Elements of the surface become helices of angle a, and a radius is rotated through an angle b in length L. The state of stress of an element from the surface is pure shear *(fig. 1C)*. Pure tension of the same magnitude as the shear stress is produced across the plane $A—A'$ at an angle of 45° with the direction of the shear stress. There is an equal compressive stress on a plane $B—B'$ at right angles to the tension plane. The stress in shear (S_s) on the outer surface of a hollow, circular cylinder in torsion is a function of the torsional moment (T) and the physical dimensions of the cylinder as follows:

$$S_s = \frac{16\,(T)\,(d_o)}{\pi(d_o^4 - d_i^4)}$$

Forgacs (3) states that ribbonlike particles are formed after propagation of cracks in the direction of the S_2 helix (angle F, fig. 1C). It is generally held that the cell wall microfibrils adhere strongly in large aggregates—termed fibrils—and that a zone of weakness exists between these aggregates. To produce the desired crack, the cell wall must be stressed in excess of the tensile or shear strength of the zone of weakness.

For a given torsional moment, shearing stresses S_s of equal magnitude are introduced parallel and perpendicular to the axis of the particle. They are accompanied by diagonal tensile (T_s) and compressive (C_s) stresses of equal magnitude.

The mode of failure for a particular fiber is probably determined in a complex interaction between the applied torque and the physical state of the tracheid, i.e., its

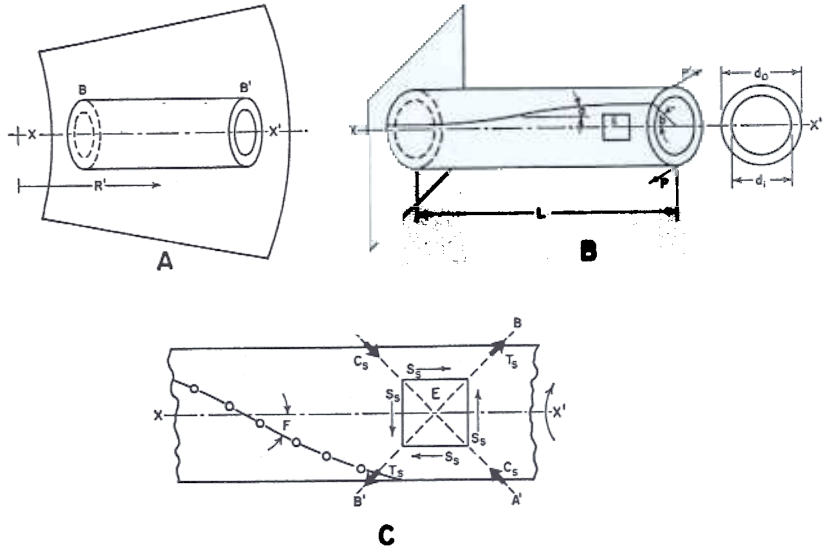

Fig. 1. Force relationships within an intact fiber during refining.

dimensions, fibril angle, and relative strengths in compression, tension, and shear. If the strength in shear parallel to the fiber axis or in diagonal tension is exceeded before the strength in diagonal compression, cracks may form parallel to the fibril helix and permit subsequent unwinding through visco-elastic deformations or pure rolling. If, however, the stress level exceeds the strength in perpendicular shear before the strengths in diagonal tension or parallel shear are exceeded, failure is likely to occur in a plane perpendicular to the longitudinal axis of the tracheid. If the strength in compression is exceeded before the strengths in parallel shear or diagonal tension, the tracheid should deform and fail by diagonal buckling.

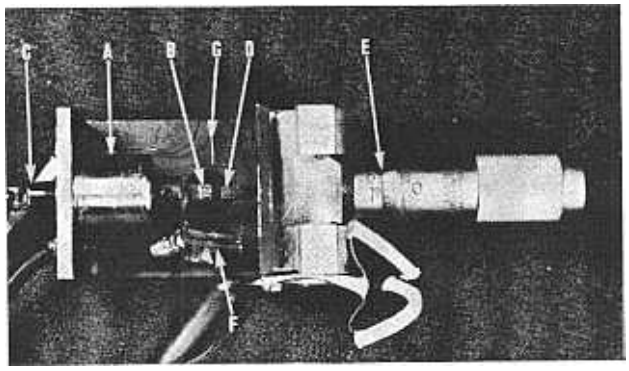

Fig. 2. Micromanipulative substage for stressing individual tracheids in torsion.

Procedure

A 300 g. sample of loblolly pine chips was available from previous research relating the effect of gross wood characteristics to the properties of handsheets made from refiner groundwood (6). The chips were dissected into earlywood and latewood fractions and macerated for 2 days in a 50/50 solution of 30-percent hydrogen peroxide and glacial acetic acid at 50°C. The wood was of a type shown to yield sheets of improved strength. The morphological data and gross wood characteristics are tabulated below; the values were obtained from matched material used in earlier work (7).

Density of unextracted material (O.D. wt. and green vol.), g/cm³	0.46
Rings per cm of growth rate	1.93
Proportion latewood	0.33
Latewood wall thickness, μm.	9.50
Earlywood wall thickness, μm.	4.36
Latewood tracheid diameter, μm.	33.30
Earlywood tracheid diameter, μm.	56.99
Latewood tracheid length, mm.	4.21
Earlywood tracheid length, mm.	3.98

After maceration and drying at room temperature, individual tracheids were carefully attached by one end to a thin strip of double-backed adhesive tape affixed along the edge of a glass slide. They were then coated with a layer of gold-palladium 200 Å thick and held in the vacuum-dry condition until tested. Preliminary tests indicated that identifiable failure types were essentially unaffected by moisture content or the gold-palladium coating.

Fig. 2 is a detailed view of the micromanipulative SEM substage designed to apply torsional stresses to single fibers. Rotary motion was provided by a miniature 50-to-1 speed reducer (A) with an anvil attached to the output shaft. The surface of the anvil (B) formed a plane passing through the axis of rotation. The anvil was rotated by a shaft (C) attached to a variable-speed, reversible DC motor outside the SEM specimen chamber. A stationary anvil was provided at position (D); its surface also formed a plane passing through the axis of rotation. The axial separation between the two members was varied by adjusting the micrometer at position (E). A miniature electrical heater (F) and thermocouple detector (G) were also incorporated in the stage design.

Tracheids were affixed to the substage by cutting the adhesive tape on either side of a fiber and pressing the tape on the extreme end surface of the stationary anvil. After the anvil had been adjusted for the desired axial separation, the opposite end of the fiber was attached to the rotating member with silver paint. Scribe lines located at the axis of rotation and a low-power light microscope aided in accurate positioning of the tracheid. All fibers were rotated in the clockwise direction at a rate of 40° per minute. Preliminary experimentation revealed that counterclockwise rotation did not produce the desired unwinding.

The scanning electron microscope was generally operated in the fast scan television mode and the image viewed on a standard television monitor at magnifications of 50 to 5,000 diameters. Video tape recordings were made for subsequent study. Hard-copy photographs were made directly from the monitor by using portions of the video tape playback. This approach was necessary because the slow scan speeds of the normal SEM display mode do not permit observation of motion without blurring of the image.

Consideration was also given to the failure characteristics of fibers pulped in a commercial double-disk refiner. Wood of the same type as previously described was used; details of the refining procedure are given in an earlier paper (6). For this portion of the study, a dilute slurry of the refined pulp was deposited on standard specimen stubs, coated with gold-palladium, and examined in the SEM by standard techniques.

Results

Because of the complexity and tedious nature of testing individual tracheids in the micromanipulative substage and because of the necessity of visually interpreting failure types, a statistical approach was not taken in evaluating the data. The results discussed here, however, are based on some 400 individual observations.

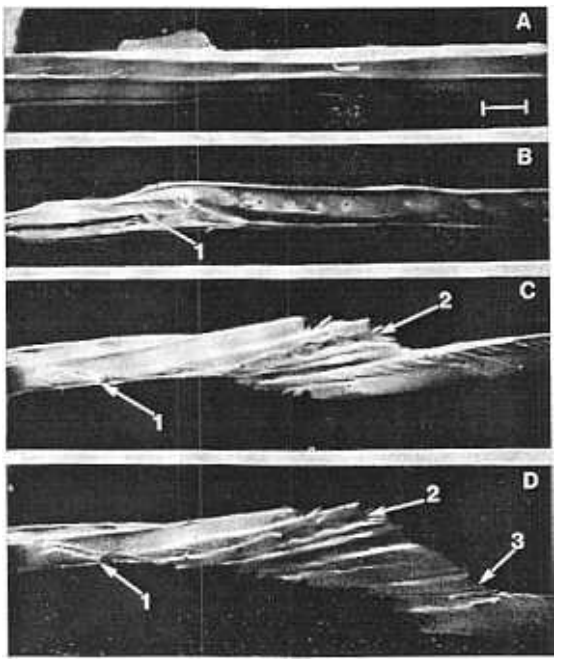

Fig. 3. Development of a Type I (unwinding) failure in an earlywood tracheid. The scale mark in A shows 50 μm and is also applicable to B, C and D.

Failure types

The three previously postulated modes of failure were identified during the course of the experiment. The first, termed failure Type I, was characterized by the progressive formation of a ribbonlike element after propagation of a crack along the fibril helix. The series of micrographs in *fig. 3* illustrates a typical Type I failure for an earlywood fiber. *Micrograph A* shows the undeformed fiber prior to application of torsional stress. As the fiber is rotated, stresses in the cell wall increase. A critical point is eventually reached where the strength of the fiber in diagonal tension or shear parallel to the longitudinal axis is exceeded and a crack abruptly forms at the zone of weakness delineated by the fibril helix (point 1 of *micrograph B*). *Fig. 4A* shows details of such a crack at greater magnification. After the initial crack, stresses in the tracheid are reduced and additional rotation is generally needed to produce further unwinding by a tearing process in a direction generally following the fibril angle. In fig. 3, the areas between points 1 and 2 of *micrograph C* and between points 2 and 3 of *micrograph D* illustrate two steps of the process. The original crack remains visible at point 1 in all micrographs of the series. With earlywood tracheids, the unwinding process frequently continued through several complete spirals around the fiber before the unsupported ribbon broke from the parent tracheid.

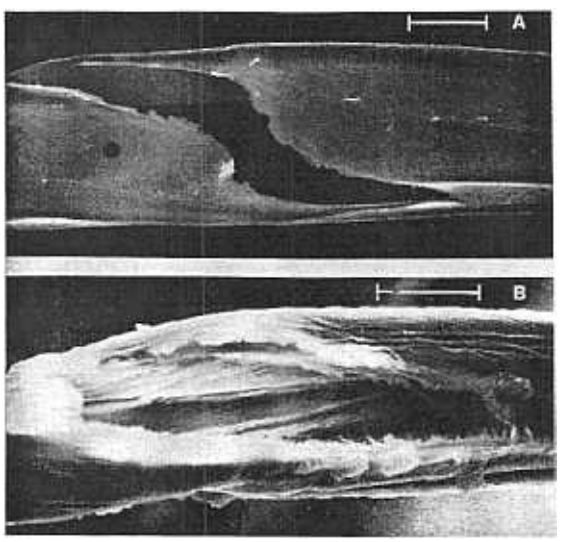

Fig. 4. Detailed view of Type I initial crack in an earlywood (A) and latewood (B) tracheid. The scale mark shows 25 μm.

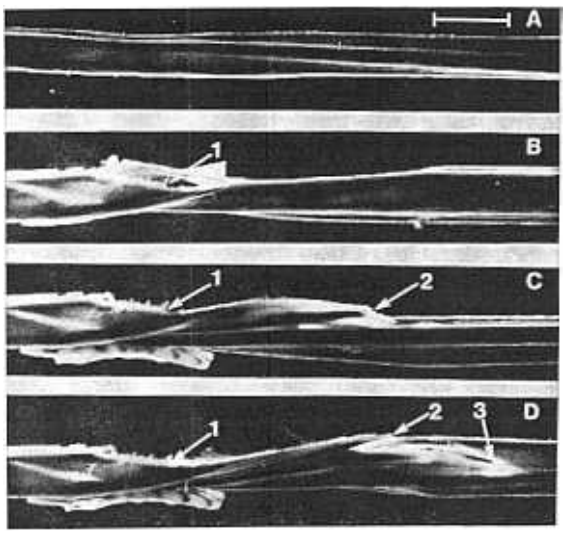

Fig. 5. Development of a Type I (unwinding) failure in a latewood tracheid. The scale mark in A shows 50 μm and is also applicable to B, C and D.

The micrographs of *fig. 5* show the formation of a typical Type I failure in a latewood tracheid. The undeformed fiber is depicted in *fig. 5A*. The formation of the initial crack is shown at point 1 in *fig. 5B* and in greater detail in *fig. 4B*. Two stages of the progressive tearing action are illustrated in *fig. 5C* between points 1 and 2 and in *fig. 5D* between points 2 and 3. The edge of the original crack remains visible at point 1. The length of the ribbonlike element was generally shorter for latewood than for earlywood fibers—usually limited to no more than one or two spirals. This observation supports the contention that the lower strength of southern pine refiner groundwood pulps is partly associated with difficulty in unwinding the thick-walled latewood fibers.

Failure Type II occurs when fibers fail in shear along a plane perpendicular to their longitudinal axis. The

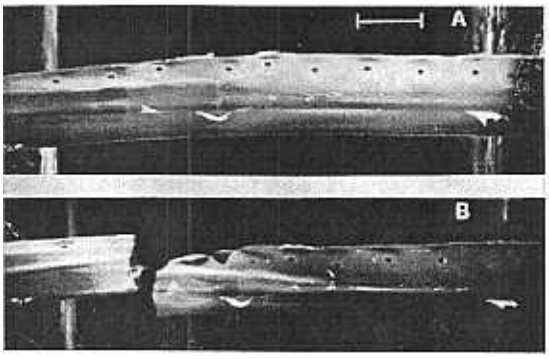

Fig. 6. Development of a Type II (shear) failure in an earlywood tracheid. The scale mark in A shows 50 μm and is also applicable to B.

micrographs of *fig. 6* show a typical Type II failure for earlywood. *Micrograph A* depicts the undeformed fiber prior to application of torsional stress. After a small amount of rotation with little or no observable twisting, strength in shear perpendicular to the longitudinal axis is exceeded and failure occurs *(fig. 6B)*.

Fig. 7 illustrates a Type II failure in latewood. With latewood, the undeformed fiber *(fig. 7A)* rotates through a considerable angle, and substantial deformation occurs *(fig. 7B)*. Eventually a critical point is reached where the strength in perpendicular shear is exceeded and the tracheid fails *(fig. 7C)*.

Type III failures were by buckling—there were no discernible differences between earlywood and latewood *(fig. 8)*. *Micrograph A* shows an undeformed tracheid. After considerable rotation, the strength of the fiber in diagonal compression is exceeded and buckling occurs *(fig. 8B)*. With further rotation, the degree of buckling increases *(fig. 8C)*, and frequently the fiber spirals around itself several times.

Type I failures are of principal interest here, since

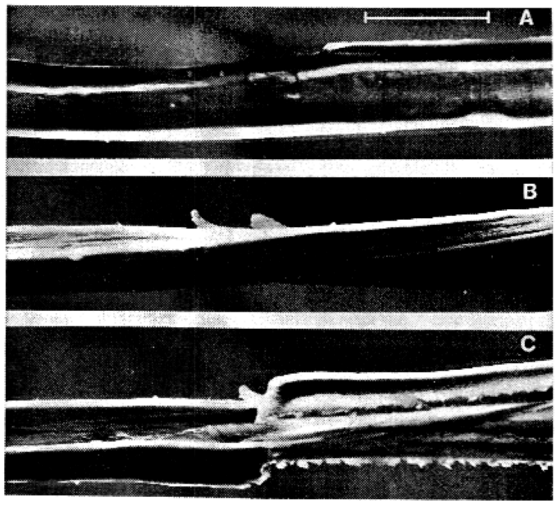

Fig. 7. Development of a Type II (shear) failure in a latewood tracheid. The scale mark in A shows 50 μm and is applicable to B and C.

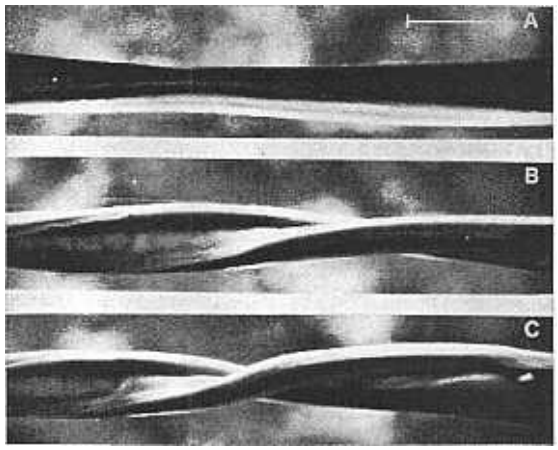

Fig. 8. Development of a Type III (buckling) failure in an earlywood or latewood tracheid. The scale mark in A shows 50 μm and is applicable to B and C.

they produce particles having improved bonding potential. Fibers exhibiting characteristics closely resembling those of the experimentally produced Type I were readily observed in southern pine pulps manufactured in a commercial double-disk refiner. *Fig. 9* is a series of micrographs of such fibers. *Micrograph A* illustrates the formation of a crack in a direction parallel to the fibril helix, while *B*, *C*, *D*, and *E* show progressive stages of unwinding into ribbonlike elements. Lastly, *F* shows an unwound ribbon draped across the surface of two intact tracheids. The readily apparent similarity to experimentally unwound fibers supports the concept that, in manufacture of conventional refiner groundwood,

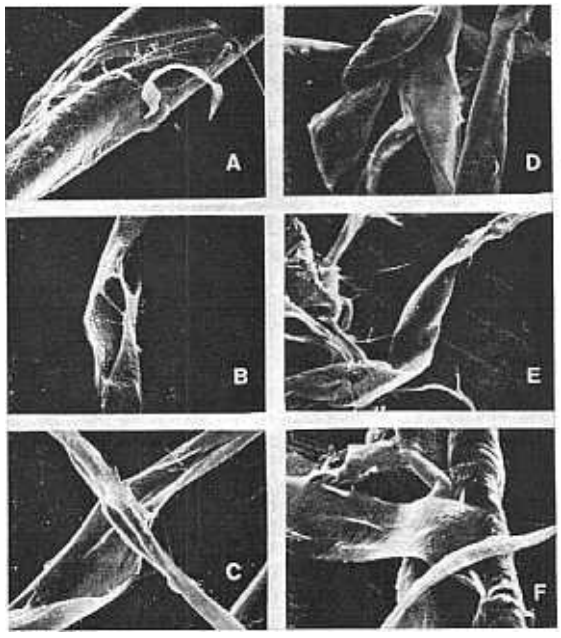

Fig. 9. Characteristic Type I failures in commercially produced southern pine refiner groundwood pulp.

ribbons are formed through an unwinding process after the tracheid is stressed in torsion.

Factors affecting failure type

The effect of axial separation (distance between the points of applied torque) and temperature on failure type was evaluated for earlywood and latewood in a factorial experiment with variables as follows:

Axial separation: 0.64, 1.27, and 2.54 mm
Temperature: 20°C and 100°C

Fifteen observations were made for each factorial combination. Failure type was noted and expressed as a proportion of the total number of observations.

Type I (unwinding) failures were most common. The average proportion was 0.75 and 0.77 for earlywood and latewood, respectively. For earlywood, the proportion of Type I failures decreased with increasing axial separation. The proportion was unaffected when tracheids were heated to 100°C. The values averaged over both temperatures were 0.87, 0.77, and 0.60 for axial separations of 0.64, 1.27, and 2.54 mm.

The proportions of Type I failure for latewood were:

Axial separation mm	*Temperature*	
	20°C	*100°C*
0.64	0.60	0.87
1.27	.67	.80
2.54	.80	.87

From the tabulation, the proportion increased with increasing axial separation when tested at 20°C, but remained relatively constant at 100°C. For a given separation, the proportion of Type I failures was greater for hot than for cold fibers.

For both earlywood and latewood, the proportion of Type II shear failures was generally greatest when the axial separation was small than when it was large. Type III buckling failures were principally associated with wide axial separation.

In the previously discussed study of commercial pulps, many intact tracheids appeared to have portions of the S_1 layer removed through an abrading or peeling process. The S_1 consists of a number of lamellae having fibrils randomly oriented with respect to the fiber axis. It seemed possible that the S_1 layer may tend to inhibit Type I failures, since torsional stresses are not directly applied to the preferential zone of weakness in the S_2 layer.

To test this concept, 15 earlywood and 15 latewood tracheids were isolated from a single-pass commercial refiner groundwood pulp. It was assumed that the S_1 layer would be absent in some specimens from this sample but present in samples prepared by maceration. The fibers were stressed in torsion at room temperature and with an axial separation of 1.27 mm.

It was found that the proportion of Type I failures was essentially the same for both samples. However, the length of ribbon formed along the direction of the fibril angle in the S_2 layer was greater for partially refined tracheids than for macerated tracheids. It is concluded that removal of the S_1 layer prior to application of torsional stresses aids the development of ribbonlike elements.

Literature

1. *Morkved, L.* and *Larson, P.:* Refiner groundwood. Tappi *52* (1969) 1465.
2. *McMillin, C.W.:* Quality of refiner groundwood pulp as related to handsheet properties and gross wood characteristics. Wood Sci. and Technol. *3* (1969) 287.
3. *Forgacs, O.L.:* The characterization of mechanical pulps. Pulp & Paper Mag. Can. *64* (1963) T89.
4. *McMillin, C.W.:* Aspects of fiber morphology affecting properties of handsheets made from loblolly pine refiner groundwood. Wood Sci. and Technol. *3* (1969) 139.
5. *Atack, D.* and *May, W.D.:* High speed photography of particle motion in a disc refiner. 2 p. in Proc. 9th Internat. Congr. High-speed Photography. Soc. Motion Picture and Television Engr. N.Y. (1970).
6. *McMillin, C.W.:* Gross wood characteristics affecting properties of handsheets made from loblolly pine refiner groundwood. Tappi *51* (1968) 51.
7. *McMillin, C.W.:* Morphological characteristics of loblolly pine wood as related to specific gravity, growth rate and distance from pith. Wood Sci. and Technol. *2* (1968) 166.

(Manuscript received October 15, 1973)